Venkateswarlu and Gunneswara Rao
Journal of Engineering and Applied Science (2023) 70:100
https://doi.org/10.1186/s44147-023-00270-0

Journal of Engineering and Applied Science

RESEARCH Open Access

Effect of steel and PVA fibres as monofibres on strength and cracking properties of fly ash and slag-based alkali-activated concrete

Mangalapuri Venkateswarlu[1*] and T. D. Gunneswara Rao[2]

*Correspondence:
mv718113@student.nitw.ac.in

[1] Research scholar, Department of Civil Engineering, National Institute of Technology, Warangal, Telangana 506004, India
[2] Professor, Department of Civil Engineering, National Institute of Technology, Warangal, Telangana 506004, India

Abstract

The present paper explores the experimental study on the influence of steel fibres (SF) and polyvinyl alcohol fibres (PVAF) as monofibres on the strength, and cracking properties of alkali-activated concrete with varying ground granulated blast furnace slag (GGBFS) and fly ash amounts was examined under ambient curing in this study. The alkali activator was a mixture of sodium hydroxide (NaOH) and sodium silicate (Na_2SiO_3) solutions. A molarity of 2 M NaOH solution and a fixed alkaline ratio (AR) of 1.5 were used in all mixes. Steel and polyvinyl alcohol (PVA) fibres were employed as monofibres. Steel fibres were added in 0.5%, 0.75%, and 1.00% volume fractions, whereas PVAF were added in 0.15%, 0.30%, and 0.45% volume fractions. In this study, a compressive strength test was performed; furthermore, a uni-axial tension test on reinforced concrete prisms was performed for tensile (first crack load, yield load, tensile stress in concrete, and tension stiffening effect) and cracking (crack spacing and crack width) properties. From the test results, better improvements in compressive strength, first crack load, yield load, tensile stress in concrete, and tension stiffening effect were observed in specimens having 1.00% steel fibres and specimens having 0.30% PVA fibres as monofibres. In the mixes containing 100% GGBFS, there was an improvement in the first crack load of approximately 46% due to 1.00% steel fibres and an approximately 29% improvement due to 0.30% PVA fibres. Furthermore, reduced crack spacings and minimum crack widths were found at 1.00% volume fraction of steel fibres and also in specimens having 0.30% PVA fibres. Overall, this study found that 1.00% steel and 0.3% PVA fibres as monofibres in fly ash-slag-based alkali-activated concrete (FSAAC) were optimal doses in terms of strength and cracking characteristics.

Keywords: Steel fibres, PVA fibres, FSAAC, Compressive strength, Tensile stress in concrete, Tension stiffening effect, Cracking pattern

Introduction

In reinforced concrete, because concrete is a brittle material, the steel member carries the majority of the tension in cracked-reinforced concrete members, while only a small quantity of concrete actually transfers the tension between the cracks. Since concrete is brittle, these cracks cannot transfer much stress across them, and as a result, once a

crack forms, the maximum tensile load of the reinforced composite is achieved at the crack, lowering the member's capacity to withstand tensile loads [1]. Furthermore, high bond stresses are required to transfer tensile loads between cracks in concrete mixtures. As a result, both load-carrying and concrete cracks contribute to the deterioration of the concrete mixture. In stiffness calculations, the contribution to stiffness made by the concrete between the cracks should be taken into account; generally, this phenomenon is called tension stiffening [2, 3].

Many investigators and practitioners in the concrete field have been interested in research on the cracking and stiffness of reinforced concrete (R.C.) components. Cracking has a remarkable effect on the stiffness and strength of R.C. elements [4]. The tension-stiffening behaviour has been determined to be important in terms of beam and slab service load performance, although it has only a minimal effect on the ultimate strength of typical R.C. members under bending or tension [5]. But when crack spacing, crack width, stiffness, and deflection characteristics of flexural and tensile elements are of concern, it also becomes a vital role in assessing serviceability requirements [2, 3, 6]. But in plain and reinforced concretes, it is a major weakness in terms of the serviceability criteria. It has been mentioned in many researches that this important weakness can be overcome by introducing various kinds of fibres in concrete mixes [7, 8]. Likewise, enhancements in tensile strength, stiffness, and improvements in cracking properties through fibre reinforcement of concrete have been investigated in many studies [9, 10]. For example, improvements in tension stiffening, smaller crack spacings and reduction in crack widths were observed in reinforced concrete by using steel fibres [3, 11]. Better improvement is achieved by reinforcing the beams and concrete prisms with steel and GFRP bars and adding steel and glass fibres [12–14]. The tension stiffening effect of glass fibre-reinforced polymer (GFRP)-reinforced concrete was studied. The results indicate the effect of concrete strength on tension stiffening loss, with higher concrete compressive strength resulting in the least decrease in concrete tensile stresses. Since the addition of steel fibres, an increase in the first crack load and yield load in steel was observed. Additionally, improvements in cracking characteristics were seen [15]. Hung et al. [16] studied how steel-reinforced ultra-high-performance concrete (UHPC) members behaved under tension in concrete ties. From the results, Steel fibre incorporation into steel-reinforced UHPC resulted in enhanced bond strength and observed a shift in failure patterns from several localised cracks to a single localised crack. The presence of fibres in concrete influences post-cracking behaviour and increases load-bearing capacity as fibre content increases; maximum load and ultimate displacements are affected by fibre content [17]. Fibre volumetric ratio, aspect ratio, fibre length, and type of fibre play a very important role in concrete properties. Increasing the fibre volumetric ratio and aspect ratio decreases the bond behaviour of the reinforced bar, so the tension-stiffening effect is reduced [18].

Engineered cementitious composites (ECCs) are now playing a significant role in the construction sector since they have several advantages from a sustainability point of view and have superior strength, durability, tensile, and cracking capabilities than normal concrete. As a result, numerous researchers have recently been experimenting with ECC-based concretes both with and without fibres. Ganesan et al. [19] noticed that geopolymer fibre-reinforced concretes (GFRCs) exhibit similar behaviour to ECCs

and display better strain hardening behaviour and greater strain capacity. Average tensile stresses and ultimate tensile strength in concrete increase even after the first crack occurs, resulting in increased bond factor values. Fischer and Li [1] and Moreno [20] examined the high-performance fibre-reinforced cement composites (HPFRCC) under tensile loading. From the results, after ECCs are substituted in brittle concretes, strain hardening and multiple cracking capabilities of HPFRC are seen. This improves tensile strength, load deformation characteristics, and energy absorption. This is due to the fact that the ECC mixture gives the member ductility properties by making the concrete stronger near cracks and between cracks. Better stress performance index and ultimate tensile strength values were observed in fly ash-based engineered geopolymer composite (EGC) and ECC mixtures by using low-concentration alkali-activated solutions [21]. Steel and basalt fibres, used as monofibres and hybrid fibres in geopolymer composites, increase tensile and cracking properties [19]. Rath et al. [22] observed various crack patterns in concrete beams with up to 50% replacement of natural fine aggregate with polyethylene terephthalate (PET) waste, both experimentally and analytically (using the ABAQUS software). Albitar et al. [23] explored the tensile and cracking characteristics of geopolymer concretes bindered with fly ash and granulated lead smelter slag (GLSS) and were compared to those of ordinary Portland cement-based concretes (OPCCs). From the results, geopolymer concretes (GPCs) exhibit better tension-stiffening properties than OPCs.

Research significance

Many studies have addressed the role of various fibres in concrete, as evidenced by the preceding literature. Many researchers have focused their efforts on the fresh and mechanical properties of alkali-activated and geopolymer composites, although both geopolymer composites and alkali-activated composites can be produced from aluminosilicate materials such as fly ash and GGBFS. However, research on fly ash-slag-based fibre-reinforced alkali-activated concrete (FSFAAC) is limited. Several investigations have been conducted on the tensile and cracking properties of OPC-based fibre-reinforced concrete (FRC), but there is less literature available on the tensile and cracking properties of FSFAAC. As a result, this investigation was carried out in alkali-activated concrete with two different fibres and varying proportions of GGBFS and fly ash to quantify the improvements in mechanical, tensile, and cracking properties. It was also investigated how fly ash, fibre type, and fibre dose affect the aforementioned qualities of FSAAC.

Experimental

Materials

GGBFS and fly ash were used in place of binding materials in this investigation. GGBFS was obtained from JSW Cement in Warangal and verified according to IS: 12,089–1987 [24]. In contrast, fly ash was collected from a thermal power station in Ramagundam, Telangana, and certified to be IS 3812–1981 [25]. Table 1 shows the physical and chemical parameters of the corresponding binding materials. The physical properties of the binder materials and aggregates are presented in Table 2. In this study, steel fibres and

Table 1 Physical properties and chemical composition of binders GGBFS and fly ash

Binder	CaO	SiO_2	Al_2O_3	Fe_2O_3	SO_3	MgO	Na_2O	LOI	Specific gravity	Specific area (m^2/kg)
GGBFS	34.21	33.46	20.40	0.8	0.9	7.77	0.13	0.38	2.9	355
Fly ash	1.82	62.32	26.53	4.22	0.37	1.03	0.21	0.86	2.11	450

Table 2 Physical properties of materials

Material	Density (kg/m^3)	Specific gravity	Specific surface area (m^2/kg)
GGBFS	1300	2.90	355
Fly ash	1200	2.11	450
Fine aggregate	1650	2.63	–
Coarse aggregate	1700	2.73	–

PVA fibres were incorporated in all the mixes, and the corresponding fibre properties are presented in Table 3 and shown in Fig. 1a.

Sodium hydroxide (NaOH) and sodium silicate (Na_2SiO_3) solutions were mixed to get the required alkali activator solution. Molarity of 2 M NaOH solution was used in all mixes B, but a fixed alkaline ratio (AR) of 1.5 and solution to binder ratio (S/B) of 0.45 were used in all mixes, which was decided by previous studies [26–28] as well as the relevant details are given in Table 2. Both samples of NaOH and Na_2SiO_3 solutions were mixed within 24 h to obtain proper mixing. Since the dissolution of sodium hydroxide in water is an exothermic reaction, it gives off a large amount of heat, which affects the properties of concrete. To prepare the NaOH solution, NaOH pellets were dissolved in drinking water.

The nominal size of the fine aggregates is taken to be 4.75 mm, which is in accordance with IS 383 (1970) [29]. Similarly, the nominal size of coarse aggregates is set at 12.5 mm, which conforms to IS 383 (1970) [29]. Fine and coarse aggregates have specific gravities of 2.63 and 2.72, respectively. For all combinations, the optimal fine aggregate-to-coarse aggregate ratio was determined to be 45%:55% of total aggregate volume. In this investigation, sulphonated naphthene-based polymers, namely Conplast SP430, were used as

Table 3 Properties of steel and PVA fibres

Properties	Details	
Type of fibre	PVA fibres	Steel fibres
Diameter	40 µm	0.5 mm
Length	12 mm	30 mm
Aspect ratio	300	60
Density (kg/m^3)	1290	7850
Specific gravity	1.26	7.85
Tensile strength (MPa)	1600	1181
Elongation (%)	7	–
Fibre type	Filament	–

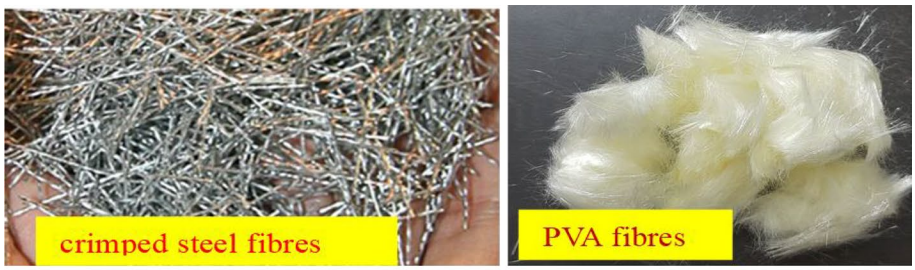

(a)

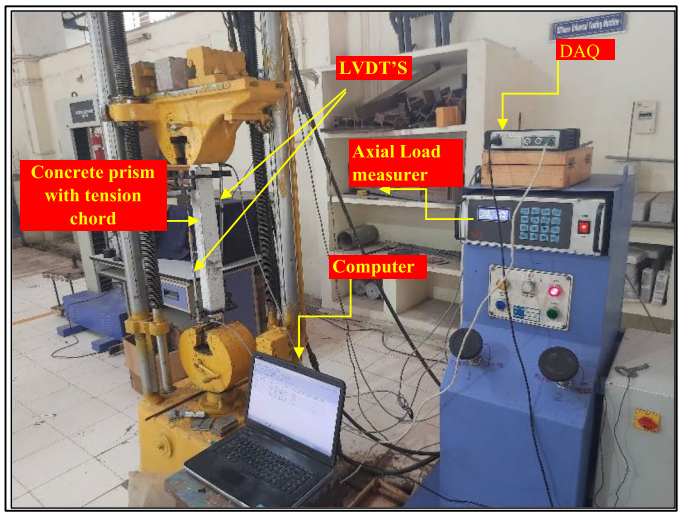

(b)

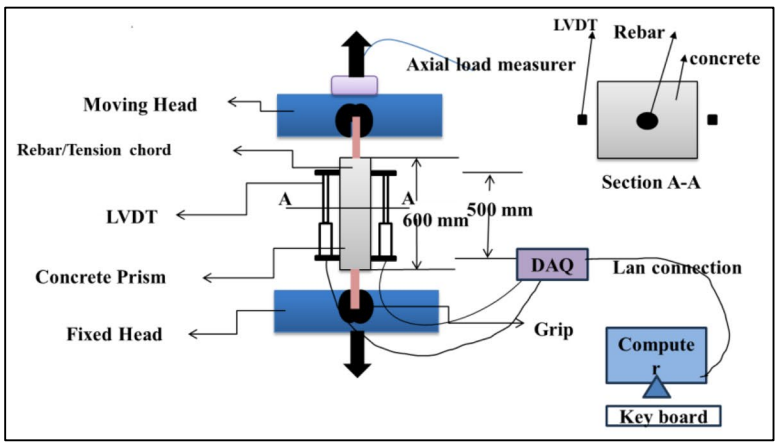

(c)

Fig. 1 Fibres and test set-ups. **a** Fibres. **b** R.C. prismatic specimen under uni-axial tension. **c** Schematic diagram for test setup

superplasticizers (SP), with this SP conforming with IS 9103–1999 [30] and BS 5075 Part 1 [31] and purchased from Fosroc Chemicals. The dosage of SP used in this study for all the mixes 6%.

Table 4 Mix proportioning of FSAAC

Mix designation (B-GGBFS/fly ash)	Binder (B)		Alkaline solution (S)		Aggregates	
	GGBFS (kg)	Fly ash (kg)	NaOH solution (kg)	Na_2SiO_3 solution (kg)	Fine aggregate (kg)	Coarse aggregate (kg)
B-100/00	400	–	72	108	819	1001
B-80/20	320	80	72	108	819	1001
B-60/40	240	160	72	108	819	1001
B-40/60	160	240	72	108	819	1001
B-20/80	80	320	72	108	819	1001
B-00/100	–	400	72	108	819	1001

Mix proportioning of FSAAC

A total of six main mixes were considered in the present study. They are Mixes B-100/00, B-80/20, B-60/40, B-40/60, B-20/80, and B-00/100. This whole mixing and proportioning took place in three stages. In the first stage, 100% GGBFS content was used in each mixture (B). Similarly, this mix is considered reference mix. Mix-B-100/00 is designed with a target compressive strength of 40 MPa and a binder material of 100% GGBFS. As part of the second stage, the GGBFS content (Mix-B) of each mix was replaced with 20%, 40%, 60%, 80%, and 100% fly ash content. Steel and PVA fibres are added as monofibres in the third stage. In volume fractions, 0.5%, 0.75%, and 1.00% steel fibres and 0.15%, 0.3%, and 0.45% PVA fibres were added separately. A total of 42 mixes were prepared. The density of alkali-activated concrete (AAC) for this mix proportioning was taken to be 2400 kg/m^3, and the mix proportioning was determined from that density, which was taken from some previous studies [28, 32]. Finally, corresponding mix proportioning details are presented in Table 4.

Sample preparation and curing

FSAAC is mixed in the same way as normal concrete [33, 34]. First, for 2–3 min, blend the binder ingredients (GGBFS and fly ash). After that, add fine and coarse aggregates to the binder material and thoroughly mix for 3–4 min. After that, an alkaline solution and superplasticizers were added. Allow for another 5–6 min of mixing to achieve a consistent and homogeneous mixture. The resultant mixture was utilised to assess the workability of the specific mix, and this concrete mixture was properly mixed again before being cast into the needed moulds. Finally, after all samples were dry, they were removed from the moulds and left to air cure at room temperature (ambient curing).

Tests performed

The slump test equipment is used to examine the workability of freshly mixed FSAAC. A steel rod was used to compact the concrete. The internal dimensions of the slump tester at the top and bottom are 100 mm and 200 mm, respectively. The cone has a height of 300 mm. This slump test was carried out in accordance with the Indian standard IS: 7320 [35]. All specimens were evaluated for 28-day compressive strength using universal testing equipment with a capacity of 1000 kN in accordance with the Indian standard 516–1959 [36]. For a flexural strength test, a three-point loading test is performed on

prisms on a digital universal testing machine. The machine has a capacity of 200 kN. This test is performed in accordance with ASTM C 293–02 [37]. Three samples were cast and tested in each proportion. Test setups are shown in Fig. 1b.

FSAAC tensile and cracking properties were studied using reinforced concrete prismatic tensile specimens (600 mm × 60 mm × 60 mm size of reinforced concrete prismatic tensile specimens). Ten-millimetre diameter high-yield strength deformed bar was used in all the specimens. All samples were tested under uniaxial tension using a universal testing machine (UTM) with a capacity of 200 kN. The change in axial length was measured using two linear variable differential transducers (LVDT) (range 100 mm, resolution 0.01 mm) positioned on opposing sides of the concrete prism during the test. Two LVDTs were used to calculate the average change in axial length. On each 1 kN load increment, crack spacing was measured. To record offset signals obtained from an LVDT, a DAQ system is used. Prior to testing, 100-mm and 20-mm grids were drawn on all sides of the sample to continuously identify crack regions during testing. Each crack's position was marked on the sample as it occurred during the test. After the test, the maximum crack width values were measured. The test sets are depicted in Fig. 1c and d. The test was carried out under load control conditions until yield. To obtain a fair bar response, naked steel bars were also tested under identical loading circumstances. Each mix had two samples tested, and the average values of the first crack load, member deformation, maximum crack spacings, and maximum crack width were recorded. Eighty-four reinforced concrete prismatic specimens were tested in this experimental programme.

Results and discussion

Compressive strength

Figure 2a and b demonstrate the variation in 28-day compressive strength caused by adding steel and PVA fibres as monofibres in various volume fractions to alkali-activated concrete with varying GGBFS and fly ash ratios.

In Fig. 2a and b, it can be observed that the 28-day compressive strength values of all the mixes increased as the GGBFS content increased from 0 to 100%. The increase in compressive strength may be due to the high calcium content of GGBFS [34, 38, 39]. Therefore, as the GGBFS content in the total binder increases, so does the availability of calcium also increases. Furthermore, the compressive strengths increased as steel

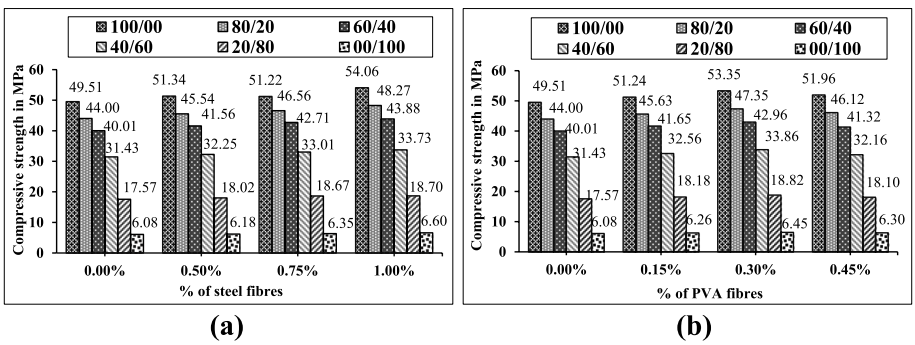

Fig. 2 Compressive strength comparison for various GGBFS and fly ash proportions and fibres. **a** Due to steel fibres. **b** Due to PVA fibres

fibres increased from 0.50 to 1.00%, and PVA fibres increased from 0.15 to 0.30%. The increased percentages of compressive strength were 3.7%, 7.49%, and 11.21% at the inclusion of 0.50%, 0.75%, and 1.00% steel fibres in B-100/00 mixes, respectively. Furthermore, improvements in compressive strengths were 3.5%, 8.09%, and 10.16% in mix B-80/20; 3.37%, 6.75%, and 9.68% in mix B-60/40; 2.61%, 5.04%, and 7.31% in mix B-40/60; 2.45%, 3.97%, and 5.84% in mix B-20/80; and 1.64%, 2.82%, and 4.93% in mix B-00/100 at the inclusion of 0.50%, 0.75%, and 1.00% steel fibres, respectively. Improvement in compressive strengths was higher in specimens having 100%, 80%, and 60% of GGBFS in mixtures, but the improvement was low at lower levels of GGBFS contents, i.e. below 40% of GGBFS. In most mixes due to adding of steel fibres, the balling effect was observed at 1.00% fibre dosage. Even though a balling effect formed, the compressive strengths improved slightly at the higher fibre dosages.

Similarly, enhancements in 28 days compressive strength were noticed to be 3.49%, 7.76%, and 4.95% at 0.15%, 0.30%, and 0.45% because of the inclusion of PVA fibre dosages in the B-100/00 mix, respectively. Also, as PVA fibres incorporated at 0.15%, 0.30%, and 0.45% percentages in the rest of the mixes, 3.70%, 7.61%, and 4.82% in mix B-80/20; 4.10%, 7.37%, and 3.27% in mix B-60/40; 3.60%, 7.73%, and 2.32% in mix B-40/60; 3.47%, 7.11%, and 3.02% in mix B-20/80; and 2.96%, 6.09%, and 3.62% in mix B-00/100 compressive strengths were observed. Similar results, i.e. 7.5% improvement in compressive strength, were noticed by Amin et al. [40] when 0.25% of 12-mm-long PVA fibres were used in OPC concrete. The improvement in compressive strengths may be due to the fibres acting as minor reinforcement against the shear forces generated by the specimen under compressive loads [41]. In all the mixtures, samples having 0.45% dosages of PVA fibres have decreased compressive strength values somewhat compared to samples having 0.30% PVA fibre dosages. Amin et al. [40] and Atahan et al. [41] also revealed the same, i.e. a higher amount of PVA fibre content decreased the compressive strength. From the previous studies' data, increasing fibres over a certain point has no positive effect on compressive strength [40, 41]. The inclusion of more PVA fibres affects vibration and consolidation [42]. Incorporation of PVA fibres in high-volume fractions results in poor dispersion of the concrete matrix [43], and thus, there is a chance of enhancing the porosity concentration in the concrete matrix [40], resulting in a weak fibre matrix interface that reduces compressive strength [21]. Overall, better compressive strengths were obtained when steel fibres were added at 1.00% and 1.25% percentages, similarly when PVA fibres were added at 0.30% percentages, and these dosages were considered optimum dosages.

Load-member strain behaviour

In the present study, load-member strain behaviour is derived from the load–displacement behaviour. This study first recorded displacement values in a R.C. prism due to applied uni-axial tensile load and the corresponding displacements considered as member displacements. Member strain values are determined from member displacements. The strain response of load-members is useful for understanding the tensile behaviour of concrete before the first crack, after the first crack (post-crack), and during the cracking in a reinforced concrete prism. Also, the load-carrying capacity of the concrete between the cracks (tension stiffening effect) due to the applied tensile load can be found through

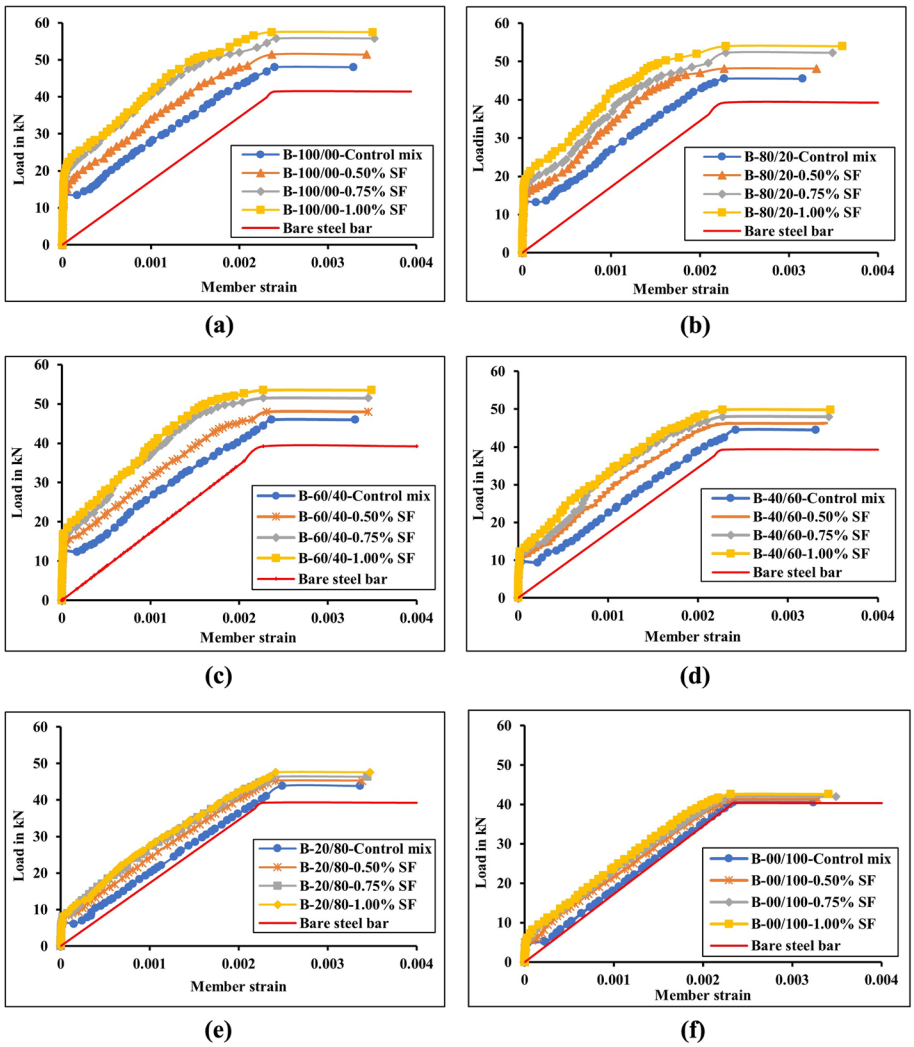

Fig. 3 Load vs. member strain behaviour due to steel fibres. **a** B-100/00. **b** B-80/20. **c** B-60/40. **d** B-40/60. **e** B-20/80. **f** B-00/100

this load-member strain response. Figure 3 shows the variations in load-member strain response caused by the addition of steel fibres at different volume fractions (0.50%, 0.75%, and 1.00%) in alkali-activated concrete with different GGBFS and fly ash ratios. Similarly, Fig. 4 demonstrated the variations in load-member strain response caused by the insertion of PVA fibres at varying volume fractions (0.15%, 0.30%, and 0.45%) in alkali-activated concrete with varied GGBFS and fly ash ratios.

In Figs. 3 and 4, as the GGBFS content in the binder increased, the load at first crack and the yield load capacity of steel in member increased. Also, the load-carrying capacity of concrete between cracks is increased. Specimens with higher amounts of GGBFS contents in the binder exhibited better strain-hardening behaviour before and after the first crack compared to specimens with lower GGBFS contents in the binder. Specimens containing 100/00, 80/20, and 60/40 GGBFS/fly ash ratios exhibited better first crack loads, yield loads, and strain hardening compared to the remaining specimens containing other GGBFS/fly ash ratios. This may be due to better binding (bond) properties

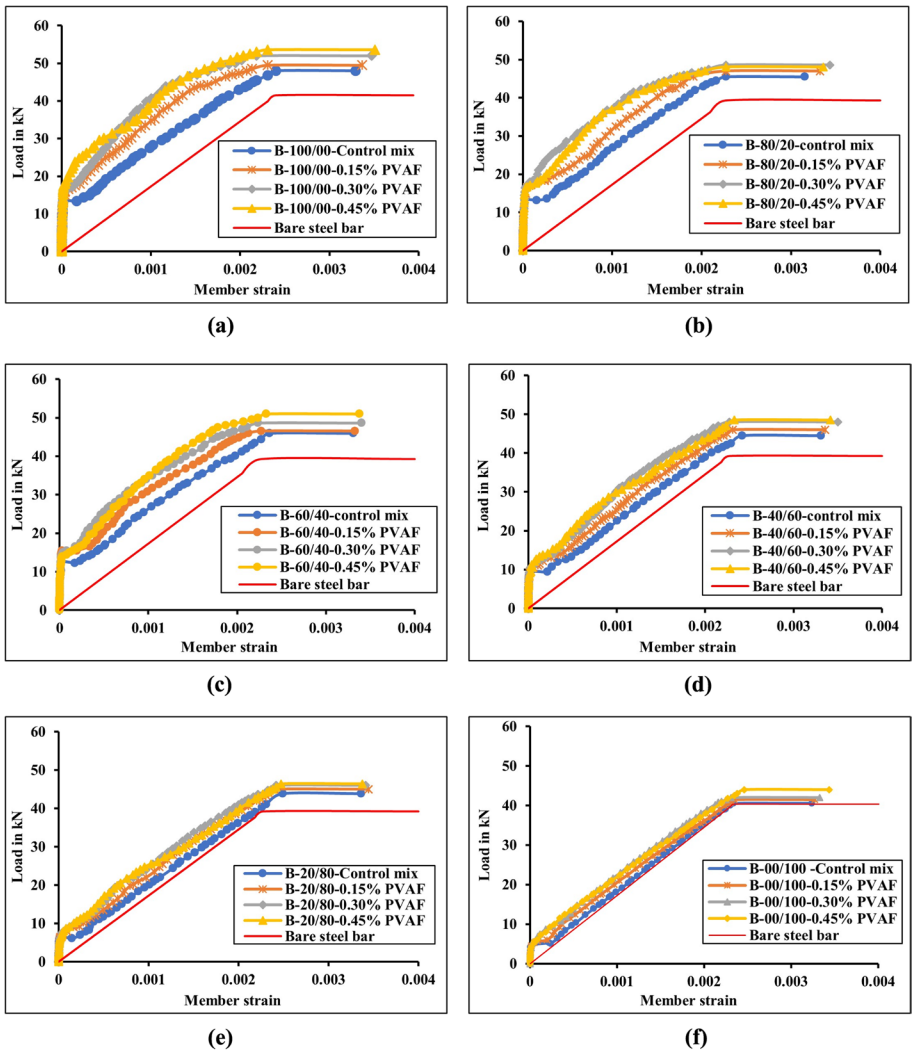

Fig. 4 Load vs. member strain behaviour due to PVA fibres. **a** B-100/00. **b** B-80/20. **c** B-60/40. **d** B-40/60. **e** B-20/80. **f** B-00/100

due to better synergy between GGBFS and fly ash binder compared to sole binder fly ash. Fischer and Li [1] and Moreno [20] also revealed that after ECCs are substituted in brittle concretes, improvements in strain hardening and multiple cracking capabilities of HPFRC were seen. This improves tensile strength, load deformation characteristics, and energy absorption. The tensile load-carrying ability of concrete between the cracks depends on the bond that existed between concrete and steel; in relation to crack spacing, it developed as member cracks [2, 44, 45]. In some specimens, the presence of high levels of fly ash in the binder did not achieve good bond properties, possibly due to the use of low-molarity NaOH solution and curing the specimens in ambient curing instead of heat curing. Heat curing is needed to get better geopolymerisation in fly ash AAC or fly ash-based GPC [27, 46]. The first crack load and yield loads and their increments due to steel fibres and PVA fibres were presented in Tables 5 and 6.

Table 5 Increments in first crack tensile load and yield load due to steel fibres

Mix designation	Volume fraction of steel fibres (%)	First crack load (kN)	% of increase in first crack load	Yield load (kN)	% of increase in yield load
B-100/00	0.00%	13.40	–	48.00	–
	0.50%	14.94	11.49	51.40	7.08
	0.75%	16.28	21.49	55.76	16.17
	1.00%	19.54	45.82	57.45	19.69
B-80/20	0.00%	13.20	–	45.50	–
	0.50%	14.47	9.62	48.10	5.71
	0.75%	15.84	20.00	52.25	14.84
	1.00%	17.85	35.23	54.00	18.68
B-60/40	0.00%	12.30	–	45.96	–
	0.50%	13.76	11.87	47.96	4.35
	0.75%	15.10	22.76	51.50	12.05
	1.00%	16.75	36.18	53.50	16.41
B-40/60	0.00%	9.40	–	44.50	–
	0.50%	10.42	10.85	46.25	3.93
	0.75%	11.00	17.02	48.00	7.87
	1.00%	12.33	31.17	49.84	12.00
B-20/80	0.00%	7.00	–	43.86	–
	0.50%	7.54	7.71	45.26	3.19
	0.75%	8.00	14.29	46.38	5.75
	1.00%	8.53	21.86	47.56	8.44
B-00/100	0.00%	5.12	–	40.50	–
	0.50%	5.46	6.64	41.30	1.98
	0.75%	5.75	12.30	42.00	3.70
	1.00%	6.10	19.14	42.60	5.19

From the load-member strain responses (Figs. 3 and 4), as the dosage of steel fibres increased from 0.50 to 1.00%, the load-carrying capacity of concrete between cracks after the first crack (post-crack behaviour) increased. The inclusion of steel fibres in AAC can remarkably improve its post-cracking performance [47]. In all the composites, better first crack load, yield load, and strain-hardening properties were observed at 1.00% dosage of steel fibres as compared to the remaining dosages of steel fibres. The increased percentage of first crack load due to the incorporation of steel fibres at 0.50%, 0.75%, and 1.00% is 11.49%, 21.49%, and 45.82% in mix B-100/00 samples, respectively. Also, when steel fibres are incorporated at 0.50%, 0.75%, and 1.00% percentages in the rest of the mixes, 9.62%, 20.00%, and 35.23% in mix B-80/20; 11.87%, 22.76%, and 36.18% in mix B-60/40; 10.85%, 17.02%, and 31.17% in mix B-40/60; 7.71%, 14.29%, and 21.86% in mix B-20/80; and 6.64%, 12.30%, and 19.14% in mix B-00/100 improvement in first crack loads were observed. Maximum improvements in yield load were observed when steel fibres were added at 1.00% dosage, i.e. 19.69% in mix B-100/00, 18.68% in B-80/20, 16.41% in B-60/40, 12.00% in B-40/60, 8.44% in B-20/80, and 5.19% in B-00/100. In all the mixes, due to the incorporation of PVA fibres, load-carrying ability of concrete between cracks increased. The load at the first crack in the concrete and the yield load capacity of steel were also increased with the addition of PVA fibres. Maximum first crack loads and maximum yield loads were obtained at 0.30% PVA fibre dosage. The

Table 6 Increments in first crack tensile load and yield load due to PVA fibres

Mix designation	Volume fraction of PVA fibres (%)	First crack load (kN)	% of increase in first crack load	Yield load (kN)	% of increase in yield load
B-100/00	0.00%	13.40	0.00	48.00	0.00
	0.15%	15.03	12.16	51.50	7.29
	0.30%	17.25	28.73	55.85	16.35
	0.45%	16.13	20.37	53.78	12.04
B-80/20	0.00%	13.20	0.00	45.50	0.00
	0.15%	14.60	10.61	49.00	7.69
	0.30%	16.65	26.14	52.60	15.60
	0.45%	15.35	17.65	50.05	10.00
B-60/40	0.00%	12.30	0.00	45.96	0.00
	0.15%	13.24	7.64	48.50	5.53
	0.30%	15.00	21.95	51.65	12.38
	0.45%	14.15	15.04	49.50	7.70
B-40/60	0.00%	9.40	0.00	44.50	0.00
	0.15%	9.85	4.79	46.00	3.37
	0.30%	10.75	14.36	47.85	7.53
	0.45%	10.40	10.64	46.45	4.38
B-20/80	0.00%	7.00	0.00	43.86	0.00
	0.15%	7.15	2.14	45.00	2.60
	0.30%	7.54	7.71	46.00	4.88
	0.45%	7.31	4.43	45.40	3.51
B-00/100	0.00%	5.12	0.00	40.50	0.00
	0.15%	5.20	1.56	41.50	2.47
	0.30%	5.50	7.42	42.00	3.70
	0.45%	5.34	4.30	41.50	2.47

increased percentage of first crack load due to the incorporation of PVA fibres at 0.15%, 0.30%, and 0.45% is 12.16%, 28.73%, and 20.37% in mix B-100/00 samples, respectively. As PVA fibres incorporated at 0.15%, 0.30%, and 0.45% percentages in the rest of the mixes, 10.61%, 26.14%, and 17.65% in mix B-80/20; 7.64%, 21.95%, and 15.04% in mix B-60/40; 4.79%, 14.36%, and 10.64% in mix B-40/60; 2.14%, 7.71%, and 4.43% in mix B-20/80; and 1.56%, 7.42%, and 4.30% in mix B-00/100 improvement in first crack loads were observed. Maximum improvements in yield load were observed when PVA fibres were added, i.e. 16.35% in mix B-100/00, 15.60% in B-80/20, 12.38% in B-60/40, 7.53% in B-40/60, 4.88% in B-20/80, and 3.70% in B-00/100. Overall, better enhancements in the load carried by the concrete between the cracks, first crack load, yield load, and better member strain hardening behaviour were obtained when steel fibres were added at 1.00%, similarly when PVA fibres were added at 0.30%.

Tensile stress in concrete

Figures 5 and 6 show the variation of tensile stress in concrete over member strain when steel fibres and PVA fibres are introduced as monofibres in different volume fractions in alkali-activated concrete with varying GGBFS and fly ash ratios.

In the Figs. 5 and 6, it is observed that compared to all the mixtures, the tensile stress in concrete increased as the GGBFS content in the binder increased. Among all samples,

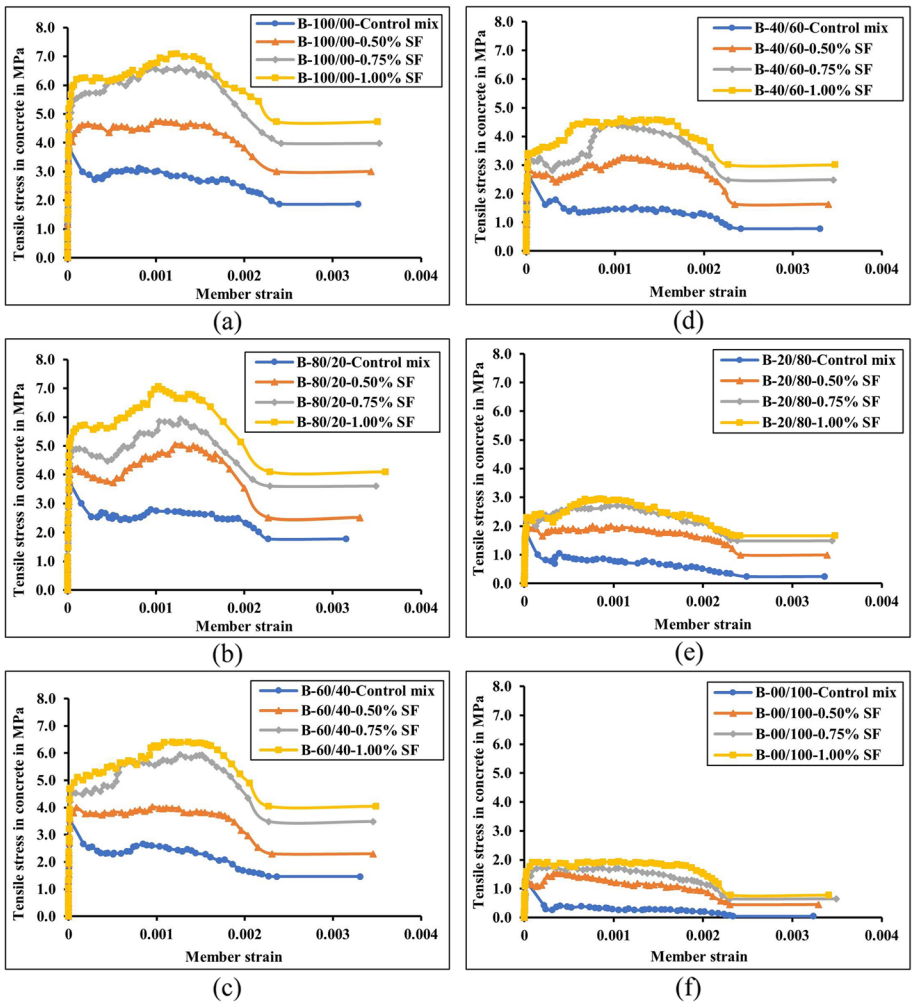

Fig. 5 Tensile stresses in concrete vs. member strain due to steel fibres. **a** B-100/00. **b** B-80/20. **c** B-60/40. **d** B-40/60. **e** B-20/80. **f** B-00/100

samples containing 100/00, 80/20, and 60/40 GGBFS/fly ash proportions exhibited maximum tensile stresses compared to the rest of the mixes. This may be due to better bonding between binder and aggregates in these mixes as compared to others. Similarly, earlier research has shown that the tension-carrying ability of concrete is affected by the bond that exists between concrete and steel [2, 44, 45]. Furthermore, due to the use of a low-concentration NaOH solution and curing conditions, specimens with high fly ash levels did not generate significant tensile stresses. When fly ash concentrations are high, high-concentration NaOH solutions and heat curing can result in greater polymerisation [27, 46] and bonding; however, low-concentration NaOH solutions and ambient curing were used in this investigation.

The tensile stresses in the concrete improved greatly by the incorporation of steel fibres and PVA fibres as mono fibres in FSAAC. When the dosage of steel fibres increased from 0.50 to 1.00%, the tensile stresses carried by the concrete between the cracks also increased compared to control mix specimens. In all mixes, specimens having steel fibres, those specimens having 1.00% steel fibres, exhibited the highest

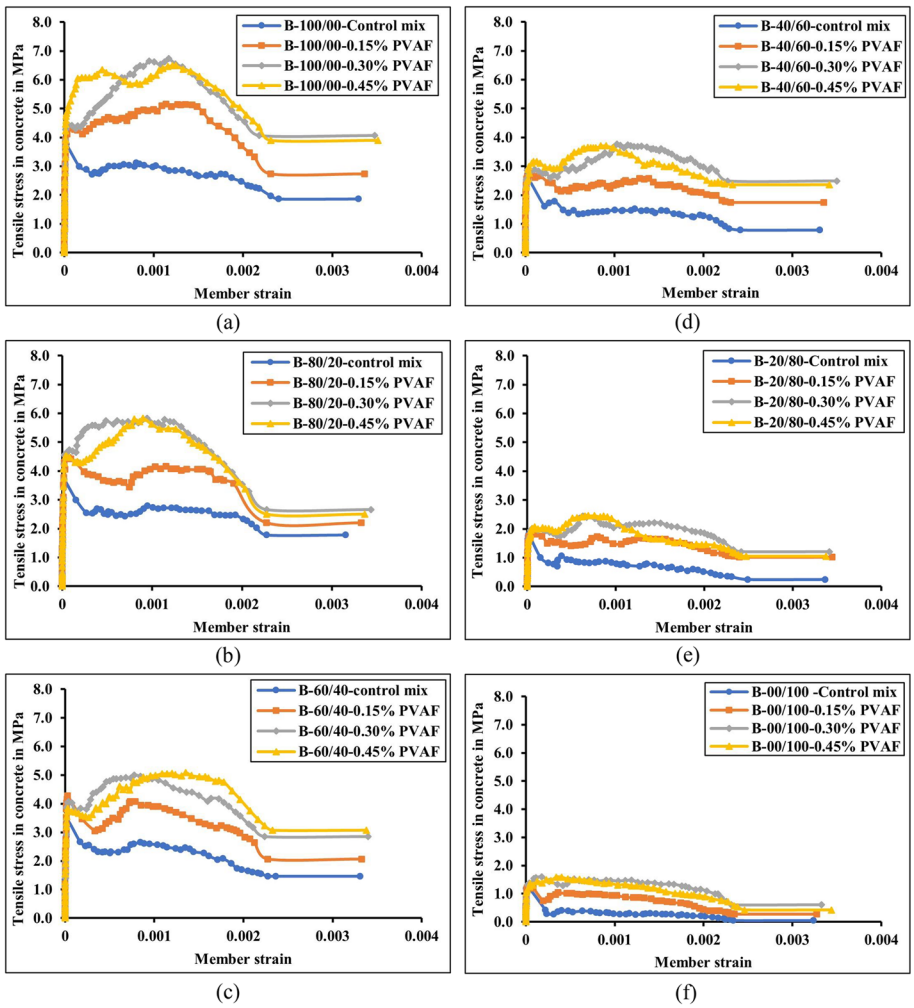

Fig. 6 Tensile stresses in concrete vs. member strain due to PVA fibres. **a** B-100/00. **b** B-80/20. **c** B-60/40. **d** B-40/60. **e** B-20/80. **f** B-00/100

tensile stress-carrying capacity and better member strain hardening behaviour before the first crack and after the first crack and also showed better post-cracking performance. The presence of fibres in concrete influences post-cracking performance and increases load-bearing capacity as fibre content increases; maximum load and ultimate displacements are affected by fibre content [17]. In most of the mixes, specimens containing 1.00% steel fibres, followed by specimens containing 0.75% steel fibres, exhibited better tensile stress-carrying capacity and better member strain hardening behaviour. The tensile stress-carrying capability of specimens containing 0.75% steel fibres was marginally lower than that of specimens containing 0.75% and 1.00% steel fibres. Among all steel fibre-containing specimens, those containing 0.50% steel fibres carried the lowest tensile stresses and exhibited low member strain hardening behaviour. Furthermore, as the dosage of PVA fibres increased from 0.15 to 0.45% the tension-carrying capacity of the concrete between the cracks also increased compared to control mix specimens. Specimens containing 0.30% PVA fibres, followed by specimens containing 0.45% PVA fibres, exhibited better tensile stress and better member

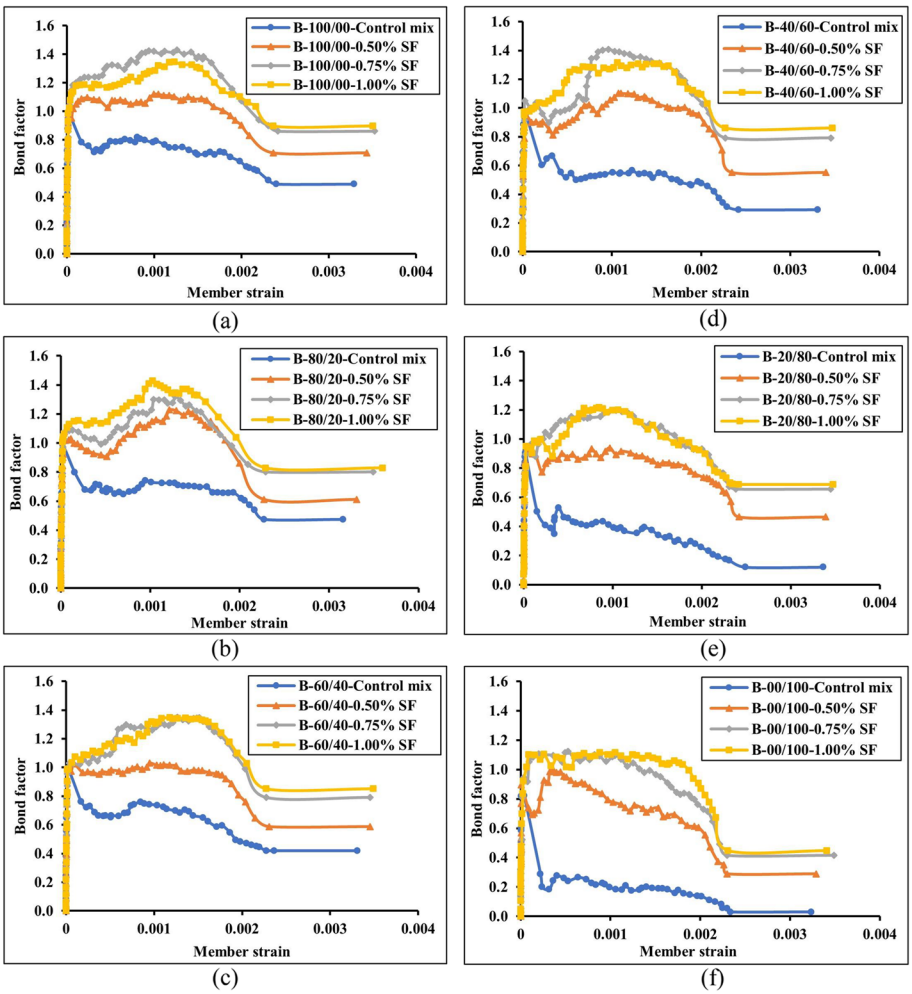

Fig. 7 Variations in tension stiffening bond factors over member stain due to steel fibres. **a** B-100/00. **b** B-80/20. **c** B-60/40. **d** B-40/60. **e** B-20/80. **f** B-00/100

strain hardening behaviour. The tensile stress-carrying ability of specimens containing 0.15% steel fibres was marginally lower than that of specimens containing 0.30% PVA fibres. Among the specimens including all PVA fibres, the specimens containing 0.15% PVA fibres displayed the least tensile stress capability and low member strain-hardening behaviour. Overall, better improvements in tensile stresses carried by the concrete between the cracks and better member stain hardening behaviour were obtained when steel fibres were added at 1.00% and 0.30% of PVA fibres as monofibres, and these dosages were considered optimum dosages.

Tension-stiffening bond factor

The bond factor or tension stiffening bond factor stated the average load carried by cracked concrete over the first cracking load in concrete between the cracks. Generally, this tension-stiffening bond factor value varies between 0 and 1. But in fibre-reinforced concrete (FRC), this tension-stiffening bond factor value exceeds 1. Figures 7 and 8

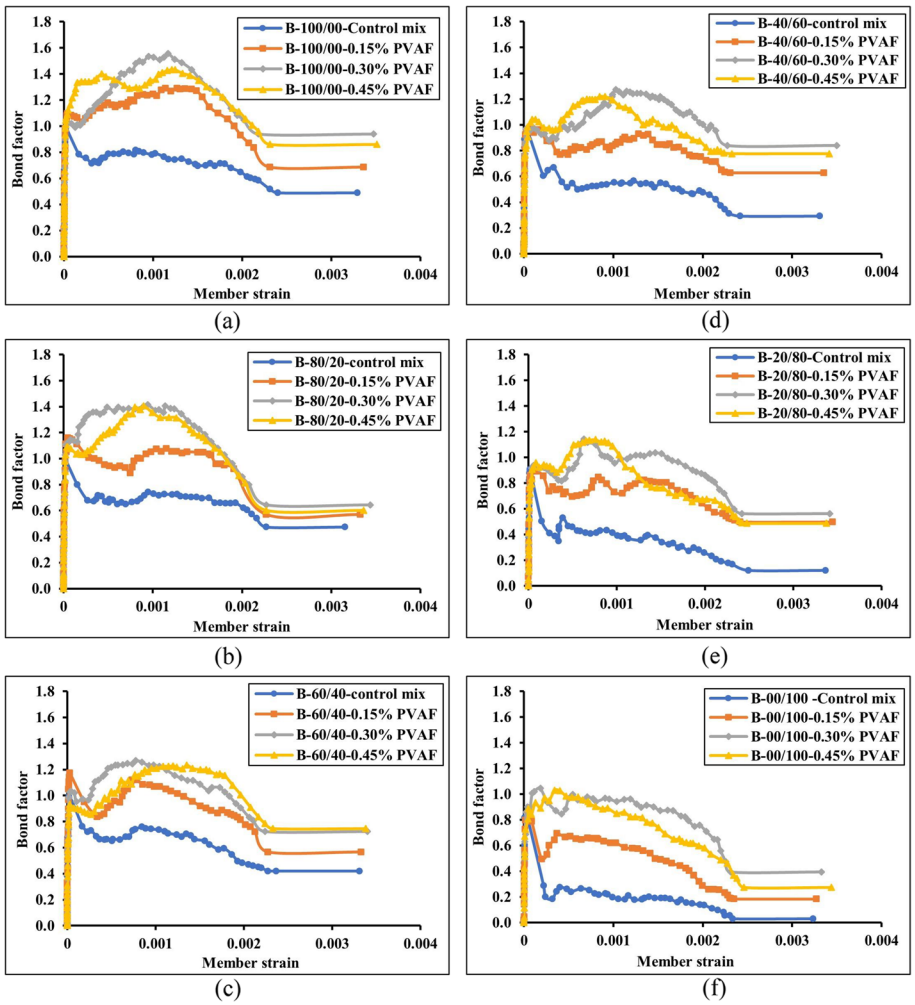

Fig. 8 Variations in tension stiffening bond factors over member stain due to PVA fibres. **a** B-100/00. **b** B-80/20. **c** B-60/40. **d** B-40/60. **e** B-20/80. **f** B-00/100

demonstrate the variation of tension-stiffening bond factor over member strain when

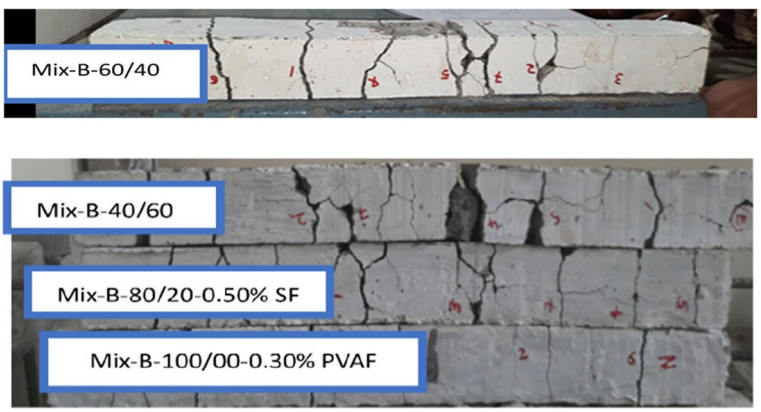

Fig. 9 Crack patterns of the specimen after testing

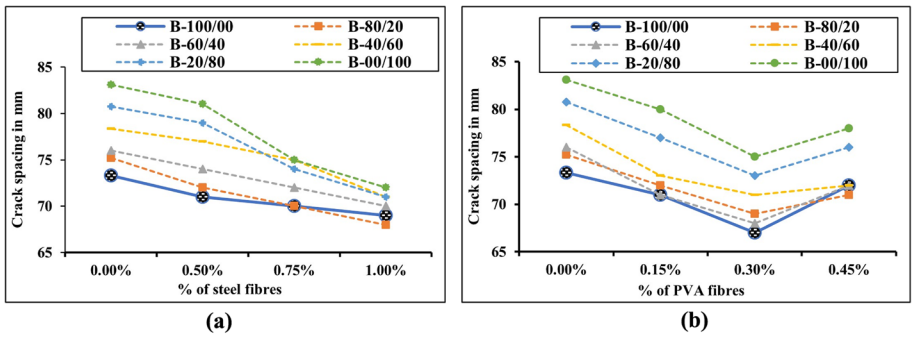

Fig. 10 Crack spacing comparison. **a** Due to steel fibres. **b** Due to PVA fibres

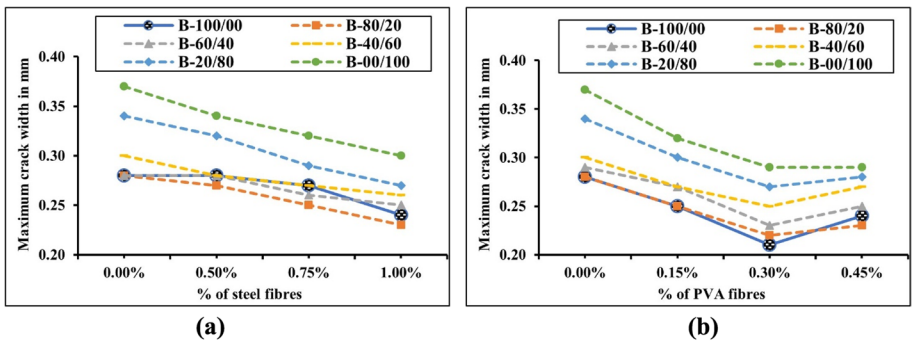

Fig. 11 Crack widths comparison. **a** Due to steel fibres. **b** Due to PVA fibres

steel fibres and PVA fibres are introduced as monofibres in different volume fractions in alkali-activated concrete with varying GGBFS and fly ash ratios.

From the Figs. 7 and 8, it is observed that compared to all the mixtures, the tension-stiffening bond factors increased as the GGBFS content in the binder increased. When 100/00, 80/20, and 60/40 GGBFS/fly ash proportions were used in alkali-activated concrete, tension-stiffening bond factors got better. This is most likely due to improved gepolymerisation at higher levels of GGBFS (despite the use of low NaOH concentrations and ambient curing), which results in greater bonding between the binder and the aggregate. In general, the tension-stiffening bond factors determine the member's stiffness during concrete cracking and after cracking. In such a scenario, a high bond factor reveals that the member's stiffness is also high, whereas a low bond factor implies that the member stiffens after the first crack and during the concrete's cracking. Similarly, previous studies have also indicated that the tension-carrying capacity of concrete between cracks (tension stiffening effect) depends on the bond between concrete and steel [2, 44, 45]. Furthermore, due to the use of a low-concentration NaOH solution and curing conditions, specimens with high fly ash levels did not generate a significant bond between concrete and steel, which yielded lower bond factors. When fly ash concentrations are high, high-concentration NaOH solutions and heat curing can result in greater polymerisation [27, 46] and bonding; however, low-concentration NaOH solutions and ambient curing were used in this investigation. The obtained bond factors are different at different GGBFS/fly ash levels, strain levels, and fibre levels, since the tension stiffening bond factor is a cracked concrete material characteristic that is independent of

the strength of the concrete and reinforcing ratio [45]. To improve the tension-stiffening effect in concrete members, various fibre types are employed. Steel and PVA fibres were employed as monofibres in this investigation to improve the tension-stiffening effect or tension-stiffening bond parameters.

The tension-stiffening bond factors in the concrete enhanced significantly by the incorporation of steel fibres and PVA fibres as monofibres. When the dosage of steel fibres increased from 0.50 to 1.00%, the tensile stresses carried by the concrete between the cracks (tension-stiffening effect) also increased. Among specimens having steel fibres, those samples having 1.00% steel fibres exhibited the highest tension stiffening bond factors before and after the first crack. Specimens containing 1.00% steel fibres, followed by specimens containing 0.75% steel fibres, exhibited better bond factors. The tensile stress-carrying capability of specimens after the first crack (tension-stiffening bond factors) containing 0.75% steel fibres was marginally lower than that of specimens containing 1.00% steel fibres. Among all steel fibre-containing specimens, those containing 0.50% steel fibres had the lowest bond factors. A maximum bond factor of 1.4 was obtained in this study at 1.00% volume fraction steel fibres used in B-100/00 and B-80/20 composite specimens. Whereas at 1.00% steel fibres volume fraction, Gribniak et al. [13] reported tension-stiffening bond factor values up to 1.4, Ganesan et al. [15] found tension-stiffening bond factor values up to 1.2 in concrete reinforced with hooked-end steel fibres. As the dosage of PVA fibres raised from 0.15 to 0.45%, the tension-stiffening effect also increased. In all mixes, specimens containing 0.30% PVA fibres, followed by specimens containing 0.45% PVA fibres, exhibited the highest tension-stiffening bond factors. The stiffness of specimens containing 0.15% steel fibres was marginally lower than that of specimens containing 0.30% PVA fibres. A maximum bond factor of 1.5 was obtained in this study at 0.30% volume fraction PVA fibres used in B-100/00 and B-80/20 composite specimens. In all mixes, the specimens having PVA fibres and the specimens containing 0.15% PVA fibres displayed the lowest bond factors. Increasing the fibre volumetric ratio and aspect ratio decreases the bond behaviour of the reinforced bar, so the tension-stiffening effect is reduced [18]. Overall, better improvements in tension stiffening bond factors (stiffness of the member) were obtained when steel fibres were added at 1.00%, similarly when PVA fibres were added at 0.30% percentages, and these dosages were considered optimum dosages.

Cracking behaviour

We are all aware that cracking behaviour (crack spacing and crack diameter) is critical when designing reinforced concrete structural members for serviceability at the limit state. These cracking behaviour concepts are more common in fibre-reinforced concretes than in ordinary concretes because long and short fibres may control crack propagation, crack widths, and crack spacing. Sometimes, these short fibres can solely arrest the micro-cracks as well. In this study, the effect of fibre type and fibre dosage on cracking (crack spacing and crack width) properties were examined. The crack formations of the failure specimens are presented in Fig. 9.

In this study, steel fibres and PVA fibres were employed as monofibres, with 0.50%, 0.75%, and 1.00% steel fibres and 0.15%, 0.30%, and 0.45% PVA fibres used, and the

experimentally obtained crack spacing and crack width results are presented in Figs. 10 and 11.

The variations in crack spacings resulting from the incorporation of steel fibres and PVA fibres in alkali-activated concrete with varying GGBFS and fly ash ratios are shown in Fig. 10. Reduced crack spacings were achieved in most composites as the GGBFS component in the total binder increased. Crack spacings were significantly reduced at 100/00, 80/20, and 60/40 GGBFS/fly ash ratios when compared to the other blends. This shows that particular mixtures produce better results in terms of serviceability. In terms of serviceability limit condition and plastic deformation factor, small crack spacing is frequently advantageous [48]. After ECC are substituted in brittle concretes, strain hardening and multiple cracking capabilities of HPFRC are seen [1, 20]. Furthermore, when steel fibres were added to all of the mixes in percentages ranging from 0.50 to 1.00%, the spacing between cracks decreased significantly when compared to the control mix specimens. Crack spacing decreased significantly as steel fibre dosage increased [15, 19]. More importantly, the lowest crack spacing was seen across all combinations at 1.00% steel fibres. This implies that the addition of fibres can influence the crack spacing. Steel fibre incorporation into steel-reinforced UHPC resulted in enhanced bond strength and observed shift in failure patterns from several localised cracks to a single localised crack [16]. Similarly, when PVA fibres were added in percentages ranging from 0.15 to 0.45%, the spacing between the cracks was greatly reduced. However, the spacing between cracks was determined to be minimal at 0.30% PVA compared to the remaining mix specimens containing steel fibres. Furthermore, the inclusion of short PVA fibres reduced crack spacing even more than the addition of steel fibres.

Figure 11 indicates that incorporating steel and PVA fibres as monofibres into concrete mixtures reduced crack widths to some extent. The tension-stiffening effect of fibre-reinforced specimens was larger than that of the control mix. This action leads to a significant reduction in steel strain, which reduces crack widths [15]. In terms of steel fibres, the crack widths were found to be reduced in specimens with 1.00% steel fibres added compared to specimens with other steel percentages added. In terms of PVA fibres, it was found that when 0.30% PVA fibres were incorporated, crack widths decreased more than in other specimens.

Conclusions

The addition of steel fibres and PVA fibres as monofibres on the strength and cracking characteristics of fly ash and slag-based alkali-activated concrete (FSAAC) cured under ambient conditions are presented in this study. This investigation revealed and determined the following significant findings:

- The compressive strength, first crack load, yield load, tensile strength, tension stiffening effect, and strain hardening behaviour increased as the GGBFS content in the total binder increased.
- The compressive strengths, modulus of rupture values, first crack load, yield load, tensile strength, tension-stiffening effect, and post-cracking behaviour of specimens increased when steel and PVA fibres were introduced as monofibres in

FSAAC at varying percentages compared to control mix specimens. Additionally, when 1.00% steel fibres and 0.30% PVA fibres were introduced as monofibres, the maximum compressive strength and modulus of rupture values were obtained in all of the mixes.

- The member's first crack load-carrying capability and yield load in steel increased more than the control mix specimens when steel and PVA fibres were added individually (monofibres).
- A significant increase in first crack load of approximately 46% was noticed in specimens having 100% GGBFS and a 1.00% volume fraction of steel fibres. Similarly, with the same steel volume fractions, the yield of steel bars in specimens increased by up to 20%. A notable increase in first crack load of approximately 29% was noticed at 0.30% volume fraction of PVA fibres and 100% GGBFS as a binder. Similarly, with the same PVA volume fractions, the yield of steel bars in specimens increased by up to 17%.
- In all mixes, specimens having 1.00% steel fibres improved their concrete's maximum tensile stress capability and tension carrying capability between cracks (tension stiffening effect). Furthermore, there were significant improvements in these values in the samples containing 0.30% PVA fibres.
- Appreciable maximum tension stiffening bond factors of 1.4 and 1.5 were observed when 1.00% steel fibres and 0.30% PVA fibres were added as monofibres in specimens with 100% GGBFS binder, respectively.
- In all mixes, specimens having 1.00% steel fibres and 0.30% PVA fibres as monofibres improved cracking problems such as crack growth propagation, crack width (minimum), and crack spacing (reduced). Something else to note about the crack problem is that shorter-length PVA fibres exhibited better crack widths and crack spacings than longer-crimped steel fibres.
- Although this study illustrates the way various monofibers affect tensile and cracking properties in detail, a detailed parametric study is required to estimate equations for crack spacing, crack width, and tension stiffening properties of plain and reinforced fly ash and slag based alkali-activated concrete tension members using other types of fibres and hybrid fibres.

Abbreviations

SF	Steel fibres
PVAF	Polyvinyl alcohol fibres
PVA	Polyvinyl alcohol
GGBFS	Ground granulated blast furnace slag
NaOH	Sodium hydroxide
Na_2SiO_3	Sodium silicate
FSAAC	Fly ash-slag-based alkali-activated concrete
R.C	Reinforced concrete
GFRP	Glass fibre-reinforced polymer
UHPC	Ultra-high-performance concrete
ECCs	Engineered cementitious composite
GFRC	Geopolymer fibre-reinforced concrete
HPFRCC	High-performance fibre-reinforced cement composites
GLSS	Granulated lead smelter slag
OPC	Ordinary Portland cement
GPC	Geopolymer concretes

AR	Alkaline ratio
SP	Superplasticizer
AAC	Alkali-activated concrete
UTM	Universal testing machine
LVDT	Linear variable differential transducer
FRC	Fibre-reinforced concrete
PET	Polyethylene terephthalate

Acknowledgements
The authors acknowledge the support from NIT Warangal and the staff members of the Material Testing and Concrete Laboratory of the Department of Civil Engineering, NIT Warangal.

Authors' contributions
Each author made significant contributions to the work's conceptualisation and design. MV and TDG conceptualised the work and developed the innovative method provided in it. MV collected the experimental data, conducted the formal analysis and interpretation of the data, and wrote and prepared the original draft. TDG reviewed, edited, and subsequently revised the manuscript. All authors have read and approved the final manuscript.

Funding
The authors declare that no funding available for this study.

Availability of data and materials
The data generated during and/or analysed during the present study are available from the corresponding author upon reasonable request.

Declarations

Ethics approval and consent to participate
This paper complied with the ethical standards of the journal.
Informed consent was obtained from all authors who contributed to the study.

Competing interests
The authors declare that they have no competing interests.

Received: 15 June 2023 Accepted: 8 August 2023
Published online: 23 August 2023

References

1. Fischer G, Victor CL (2002) Influence of matrix ductility on tension-stiffening behavior of steel reinforced engineered cementitious composites (ECC). Struct J 99(1):104–111. https://doi.org/10.14359/11041
2. Bischoff PH (2001) Effects of shrinkage on tension stiffening and cracking in reinforced concrete. Can J Civil Eng 28(3):363–374. https://doi.org/10.1139/l00-117
3. Bischoff PH (2003) Tension stiffening and cracking of steel fibre-reinforced concrete. J Mater Civil Eng 15(2):174–182. https://doi.org/10.1061/(ASCE)0899-1561(2003)15:2(174)
4. Christiansen MB, Nielsen MP (2001) Plane stress tension stiffening effects in reinforced concrete. Mag Concr Res 53(6):357–365. https://doi.org/10.1680/macr.2001.53.6.357
5. Gilbert RI, Warner RF (1978) Tension stiffening in reinforced concrete slabs. J Struct Div 104(12):1885–1900. https://doi.org/10.1061/JSDEAG.0005054
6. Ian Gilbert R (2007) Tension stiffening in lightly reinforced concrete slabs. J Struct Eng 133(6):899–903. https://doi.org/10.1061/(ASCE)0733-9445(2007)133:6(899
7. Naaman AE (1985) Fibre reinforcement for concrete. Concrete Int Des Construct. 7(3):21–25 (13)
8. American Concrete Institute (1996) ACI Committee 544 State-Of-The-Art Report on Fibre Reinforced Concrete. American Concrete Institute, Farmington Hills, MI, USA
9. Bencardino F, Rizzuti L, Spadea G, Swamy RN (2008) Stress-strain behavior of steel fibre reinforced concrete in compression. J Mater Civil Eng 20(3):255–263. https://doi.org/10.1061/(ASCE)0899-1561(2008)20:3(255)
10. ACI Committee 544 (1982) State of the art report of fibre reinforced concrete. Concrete Int Des Construct. 4(5):9–30
11. Deluce JR, Vecchio FJ (2013) Cracking behavior of steel fibre-reinforced concrete members containing conventional reinforcement. ACI Struct J 110(3). https://doi.org/10.14359/51685605
12. Bischoff PH, Paixao R (2004) Tension stiffening and cracking of concrete reinforced with glass fibre reinforced polymer (GFRP) bars. Can J Civ Eng 31(4):579–588. https://doi.org/10.1139/l04-025
13. Gribniak V et al (2013) Comparative analysis of deformations and tension-stiffening in concrete beams reinforced with GFRP or steel bars and fibres. Composites Part B: Eng 50:158–170. https://doi.org/10.1016/j.compositesb.2013.02.003
14. Vilanova I et al (2014) Experimental study of tension stiffening in GFRP RC tensile members under sustained load. Eng Struct 79:390–400. https://doi.org/10.1016/j.engstruct.2014.08.037
15. Ganesan N, Indira PV, Santhakumar A (2014) Influence of steel fibres on tension stiffening and cracking of reinforced geopolymer concrete. Mag Concrete Res 66(6):268–276. https://doi.org/10.1680/macr.13.00273
16. Hung CC, Lee HS, Chan SN (2019) Tension-stiffening effect in steel-reinforced UHPC composites: constitutive model and effects of steel fibres, loading patterns, and rebar sizes. Composites Part B: Eng 158:269–278. https://doi.org/10.1016/j.compositesb.2018.09.091

17. Di Carlo F, Spagnuolo S (2019) Cracking behavior of steel fibre-reinforced concrete members subjected to pure tension. Struct Concrete 20(6):2069–2080. https://doi.org/10.1002/suco.201900048
18. Lee SC, Cho JY, Vecchio FJ (2013) Tension-stiffening model for steel fibre-reinforced concrete containing conventional reinforcement. ACI Struct J 110(4). https://doi.org/10.14359/51685749
19. Ganesan N, Sahana R, Indira PV (2017) Effect of hybrid fibres on tension stiffening of reinforced geopolymer concrete. Advances in concrete construction 5(1):075. https://doi.org/10.12989/acc.2017.5.1.075
20. Moreno DM et al (2014) Tension stiffening in reinforced high performance fibre reinforced cement-based composites. Cement Concrete Composites 50:36–46
21. Nematollahi B, Sanjayan J, Shaikh FUA (2015) Tensile strain hardening behavior of PVA fibre-reinforced engineered geopolymer composite. J Mater Civ Eng 27(10):04015001. https://doi.org/10.1061/(ASCE)MT.1943-5533.0001242
22. Rath B et al (2022) A study on structural behaviour of CFRP laminated concrete beam with partial replacement of fine aggregate by PET granules. J Build Pathol Rehabil 7(1):58. https://doi.org/10.1007/s41024-022-00202-0
23. Albitar M, Mohamed Ali MS, Visintin P (2018) Evaluation of tension-stiffening, crack spacing and crack width of geopolymer concretes. Constr Build Mater 160:408–414. https://doi.org/10.1016/j.conbuildmat.2017.11.085
24. IS: 12089. (1987). Specification for granulated slag for the manufacture of Portland slag cement.
25. IS 3812 (Part 1) (2003) Indian standard pulverized fuel ash specification part 1 for use as Pozzolana in Cement, Cement Mortar and Concrete
26. Phoo-ngernkham T, Maegawa A, Mishima N, Hatanaka S, Chindaprasirt P (2015) Effects of sodium hydroxide and sodium silicate solutions on compressive and shear bond strengths of FA–GBFS geopolymer. Constr Build Mater 91:1–8. https://doi.org/10.1016/j.conbuildmat.2015.05.001
27. Singh SP, Murmu M (2017) Effects of curing temperature on strength of lime-activated slag cement. Int J Civil Eng 15(4):575–584. https://doi.org/10.1007/s40999-017-0166-y
28. Thunuguntla CS, Gunneswara Rao TD (2018) Mix design procedure for alkali-activated slag concrete using particle packing theory. J Mater Civil Eng 30(6):04018113. https://doi.org/10.1061/(ASCE)MT.1943-5533.0002296
29. IS 383 (2016) Indian standard coarse and fine aggregate for concrete, Bureau of Indian Standards
30. IS 9103 (1999) Indian standard concrete admixtures – specification
31. British Standard BS 5075-1:1982 (1982) Concrete admixtures. Specification for accelerating admixtures, retarding admixtures and water reducing admixtures (London: Britsh Standard Institution)
32. Thunuguntla CS, Gunneswara Rao TD (2018) Appraisal on strength characteristics of alkali-activated GGBFS with low concentrations of sodium hydroxide. Iran J Sci Technol Transact Civil Eng 42(3):231–243. https://doi.org/10.1007/s40996-018-0113-4
33. Nath P, Sarker PK (2014) Effect of GGBFS on setting, workability and early strength properties of fly ash geopolymer concrete cured in ambient condition. Construct Build Mater 66:163–171. https://doi.org/10.1016/j.conbuildmat.2014.05.080
34. Fang G, Ho WK, Tu W, Zhang M (2018) Workability and mechanical properties of alkali-activated fly ash-slag concrete cured at ambient temperature. Constr Build Mater 172:476–487. https://doi.org/10.1016/j.conbuildmat.2018.04.008
35. IS 7320:1974 (1974) Specifications for Concrete Slump Test Apparatus (4th revision). Reaffirmed-Dec 2013, BIS, New Delhi, India
36. BIS, IS (1959) IS 516–1959: method of tests for strength of concrete. Bureau of Indian Standards, New Delhi, India
37. ASTM C-293–02 (2002) Standard test method for flexural strength of concrete (using simple beam with center-point loading), International Standard Organization
38. Mallikarjuna Rao G, Gunneswara Rao TD (2015) Final setting time and compressive strength of fly ash and GGBS-based geopolymer paste and mortar. Arabian J Sci Eng 40(11):3067–3074. https://doi.org/10.1007/s13369-015-1757-z
39. Hu Y, Tang Z, Li W, Li Y, Tam VW (2019) Physical-mechanical properties of fly ash/GGBFS geopolymer composites with recycled aggregates. Constr Build Mater 226:139–151. https://doi.org/10.1016/j.conbuildmat.2019.07.211
40. Mydin MAO, Soleimanzadeh S (2012) Effect of polypropylene fibre content on flexural strength of lightweight foamed concrete at ambient and elevated temperatures. Adv Appl Sci Res 3(5):2837–2846. https://doi.org/10.4028/www.scientific.net/AMR.626.594
41. Atahan HN, Pekmezci BY, Tuncel EY (2013) Behavior of PVA fibre-reinforced cementitious composites under static and impact flexural effects. J Mater Civ Eng 25(10):1438–1445. https://doi.org/10.1061/(ASCE)MT.1943-5533.0000691
42. Noushini A, Samali B, Vessalas K (2013) Effect of polyvinyl alcohol (PVA) fibre on dynamic and material properties of fibre reinforced concrete. Constr Build Mater 49:374–383. https://doi.org/10.1016/j.conbuildmat.2013.08.035
43. Soulioti DV, Barkoula NM, Paipetis A, Matikas TE (2011) Effects of fibre geometry and volume fraction on the flexural behaviour of steel-fibre reinforced concrete. Strain 47:e535–e541. https://doi.org/10.1111/j.1475-1305.2009.00652.x
44. Kaklauskas G, Gribniak V, Bacinskas D, Vainiunas P (2009) Shrinkage influence on tension stiffening in concrete members. Eng Struct 31(6):1305–1312. https://doi.org/10.1016/j.engstruct.2008.10.007
45. Fields K, Bischoff PH (2004) Tension stiffening and cracking of high-strength reinforced concrete tension members. ACI Struct J 101(4):447–456. https://doi.org/10.14359/13330
46. Mallikarjuna Rao G, Gunneswara Rao TD, Siva Nagi Reddy M, Rama Seshu D (2019) A study on the strength and performance of geopolymer concrete subjected to elevated temperatures. In: Recent Advances in Structural Engineering, Volume 1. Springer, Singapore, pp 869–889. https://doi.org/10.1007/978-981-13-0362-3_70
47. Bernal S et al (2010) Performance of an alkali-activated slag concrete reinforced with steel fibres. Construct Build Mater 24(2):208–214. https://doi.org/10.1016/j.conbuildmat.2007.10.027
48. Zwicky D (2013) Bond and ductility: a theoretical study on the impact of construction details–part 2: structure-specific features. Adv Concrete Construct 1(2):137. https://doi.org/10.12989/acc.2013.1.1.103

Publisher's Note